PHYSICAL REVIEW D VOLUME 17, NUMBER 3 1 FEBRUARY 1978

Structure of tensor-exchange amplitudes and polarization of $\pi^- + p \to \eta + n$ †

A. P. Contogouris and M. Svec
Department of Physics, McGill University, Montreal, Canada
(Received 16 May 1977)

The structure of amplitudes of $\pi^- p \to \eta n$ is investigated by two methods: (a) fixed-t dispersion relations and effective Regge parametrization of the high-energy imaginary parts and (b) two Regge poles and finite-energy sum rules. In both cases the resulting imaginary part of the nonflip amplitude deviates from the dual-absorptive-model form. Similarities with the conclusions of other amplitude analyses involving tensor exchange are discussed. The question of A_2-ρ exchange degeneracy is also investigated. An important outcome of the work is that both methods (a) and (b) require a $\pi^- p \to \eta n$ polarization of very small magnitude throughout.

I. INTRODUCTION

For quite some time there has been much interest in the t structure of the amplitudes of two-body nondiffractive reactions. Concerning the t-channel vector exchange (odd signature) direct and detailed information is available, so that it can be said that the structure of the s-channel helicity amplitudes (SHA) is fairly well established. However, concerning the tensor exchange (even signature) the information is less direct and a number of important questions remain open.[1]

One of these questions is whether the imaginary part of the nonflip SHA has the structure predicted by the dual absorptive model (DAM), i.e., of the Bessel-function form $J_0(R\sqrt{-t})$ with $R \simeq 1$ fermi; and there has been much evidence to the contrary from amplitude analyses involving exchange with the quantum numbers of f_0,[2,3,4] of K^{**}, (Refs. 5, 6, 7) and of A_2.[8,9,10] Another important question is whether the imaginary parts of the SHA for vector and tensor exchange (such as ρ and A_2) satisfy exchange degeneracy (EXD); and the results of various investigations are very controversial.[11]

The most appropriate reaction to obtain information on tensor exchange is $\pi^- p \to \eta n$, which is dominated by purely A_2. Data on this reaction at not too high energies ($\lesssim$20 GeV) have already been exploited in amplitude analysis, together with KN charge exchange.[8] More recently[12] the differential cross sections for $\pi^- p \to \eta n$ have been determined with great accuracy up to 200 GeV, i.e., in a range of energies extending over two orders of magnitude.

For these reasons in the present work we undertook a detailed study of the amplitudes of $\pi^- p \to \eta n$. Unfortunately, for this reaction a complete set of observables (in the sense of πN reactions) is still lacking: experimental information about the spin rotational parameter T (or R)[13] is absent. Even if precise information on T existed, an overall arbitrary t-dependent phase of the amplitudes would still remain. Thus a completely model-independent analysis is not possible.

To restrict the uncertainties as much as possible we have proceeded by two somewhat different methods:

(a) The first is based on fixed-t dispersion relations (DR) together with a simple parametrization of the imaginary parts of the SHA [Eq. (2.5)]. The parametrization amounts to using one effective Regge trajectory. This method has been tested in $\pi^- p \to \pi^0 n$ (Ref. 4) and has provided one of the first amplitude analyses of $\gamma p \to \pi^0 p$ (Ref. 14) as well as information on the SHA of other reactions.[7,10,15,16]

(b) The second method makes use of two Regge poles, one with a higher trajectory (A_2) and another with a lower-lying one (say A_2'); in addition, the method relies on good satisfaction of finite-energy sum rules (FESR) (in the present work exact satisfaction for the lowest moment). The whole approach is similar to that of Barger and Phillips, which successfully predicted the polarization of $\pi^- p \to \pi^0 n$ (ρ and ρ').[17,18]

An important outcome of our work is that both methods (a) and (b) lead to real solutions for the residue functions (see Secs. II and III) only if the polarization P in $\pi^- p \to \eta n$ is of very small magnitude for all t in $0 < |t| \lesssim 1$ GeV. All the existing high-energy data are consistent with small $|P|$ (Refs. 19–21); however, the present uncertainties do not allow a firm conclusion.

Section II presents our amplitude analysis using method (a), or the one-effective-trajectory approach (OETA), and Sec. III that using method (b), or the two-Regge-poles approach (TRPA). Section IV discusses the similarities of the results of the two methods, concerning the structure of the SHA, as well as the similarities with the results of other amplitude analyses. In Sec. IV we also pre-

sent our conclusions concerning the A_2-ρ EXD question. Section V presents our predictions for the spin rotational parameter T and shows a way to experimentally distinguish between certain results of method (a) and of method (b). We conclude with certain remarks on the fact that both our methods imply $|P|$ small.

II. THE ONE-EFFECTIVE-TRAJECTORY APPROACH (OETA)

In this section we present our basic formalism for the reaction $\pi^- p \to \eta n$. We denote by $A(\nu, t)$ and $B(\nu, t)$ the usual invariant amplitudes and

$$\nu = \frac{s-u}{4M} = E + \frac{t - m^2 + \mu^2}{4M}, \tag{2.1}$$

where M, m, and μ are the nucleon, η-meson, and pion masses and E is the pion laboratory energy. Above ~2 GeV, to a good approximation, the s-channel helicity-nonflip and helicity-flip amplitudes are, respectively, given by the following two combinations of A and B:

$$M_0 = 2M(A + \nu B), \quad M_1 = \sqrt{-t}\,A. \tag{2.2}$$

Then the differential cross section and polarization are given by

$$\begin{aligned} 96\pi M^2 \nu^2 \frac{d\sigma}{dt} &= |M_0|^2 + |M_1|^2, \\ 48\pi M^2 \nu^2 P \frac{d\sigma}{dt} &= \mathrm{Im}(M_0 M_1^*). \end{aligned} \tag{2.3}$$

In view of (2.2) the amplitudes M_n, $n = 0, 1$, are crossing-even and satisfy fixed-t DR [the same as of $A(\nu, t)$]. These are of the form (leaving out, for the moment, the question of subtractions and pole contributions)

$$\mathrm{Re}M_n(\nu, t) = \frac{1}{\pi} \mathrm{P} \int d\nu' \,\mathrm{Im}\, M_n(\nu', t) \left(\frac{1}{\nu' - \nu} + \frac{1}{\nu' + \nu} \right). \tag{2.4}$$

Following usual procedures[14,4,10] we split the dispersion integrals into two pieces: a low-energy piece ($\nu \leq N$) and a high-energy one ($\nu > N$).

In the low-energy piece we calculate $\mathrm{Im}\, M_n(\nu, t)$ by means of phase-shift analysis. Thus the limit N is specified in terms of (2.1) by the limiting energy E of the phase-shift analysis.

In the high-energy piece we adopt the following effective Regge parametrization:

$$\mathrm{Im}\, M_n(\nu, t) = b_n(t)(\nu^2 - \bar{\nu}^2)^{\alpha_n(t)/2} \quad (\nu \geq N). \tag{2.5}$$

Here $\bar{\nu}$ is the unitarity threshold given by

$$\bar{\nu} = \mu + \frac{t - m^2 + \mu^2}{4M}, \tag{2.6}$$

where m and μ are the η and pion masses, and $\alpha_n(t)$ are effective Regge exponents.

Clearly, $\mathrm{Im}\, M_n$ of (2.5) represent effective A_2 (tensor) contributions; and as we discuss below, at least for small $|t|$, $\alpha_n(t)$ are not far from the experimental A_2 Regge-pole trajectory.[12] It is then easy to see that the DR (2.4) requires a subtraction. To this purpose it is convenient to introduce the asymptotic form[10]

$$M_n^{\mathrm{asy}}(\nu, t) = b_n(t) \left[-\cot \frac{\pi \alpha_n(t)}{2} + i \right] (\nu^2 - \bar{\nu}^2)^{\alpha_n(t)/2} \tag{2.7}$$

so that, for $\nu > N$, $\mathrm{Im}\, M_n^{\mathrm{asy}} = \mathrm{Im}\, M_n$. Then we can write an unsubtracted DR for the difference $M_n - M_n^{\mathrm{asy}}$; and applying well-known Hilbert transforms to the high-energy piece ($\nu > N$) of the dispersion integrals (see, e.g., the Appendix of Ref. 14) we finally obtain

$$\mathrm{Re}M_n(\nu, t) = \mathrm{Re}M_n^{\mathrm{asy}}(\nu, t) + \frac{2\nu_N r_n}{\nu_N^2 - \nu^2} + \frac{2}{\pi} \int_{\bar{\nu}}^{N} d\nu' \,\mathrm{Im}\, M_n(\nu', t) \frac{\nu'}{\nu'^2 - \nu^2} - \frac{2}{\pi} b_n(t) \int_{\bar{\nu}}^{N} d\nu' (\nu'^2 - \bar{\nu}^2)^{\alpha_n/2} \frac{\nu'}{\nu'^2 - \nu^2}. \tag{2.8}$$

The second term in the right-hand side (RHS) is the nucleon-pole contribution so that

$$\nu_N = \frac{t - m^2 - \mu^2}{4M}; \tag{2.9}$$

the residues r_0 and r_1 are given by

$$r_0 = \sqrt{2}\, g_\pi g_\eta \nu_B, \quad r_1 = 0, \tag{2.10}$$

where g_π and g_η are the πN and ηN coupling constants.[22]

In the last three terms of the RHS of (2.7) we can make an expansion in powers of $(\nu^2 - \bar{\nu}^2)^{-1}$, so that (2.7) takes the form

$$\mathrm{Re}M_n(\nu, t) = \mathrm{Re}M_n^{\mathrm{asy}}(\nu, t) + \sum_{k=0}^{\infty} (\nu^2 - \bar{\nu}^2)^{-k-1} \left[\frac{2}{\pi} \frac{b_n(t)}{\alpha_n + 2 + 2k} (N^2 - \bar{\nu}^2)^{\alpha_n/2 + 1 + k} - S_n^{(k)}(t) \right], \tag{2.11}$$

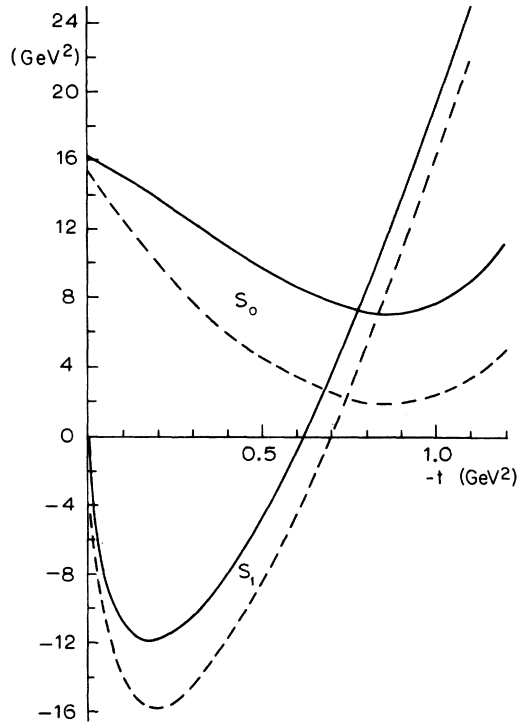

FIG. 1. The auxiliary functions $S_n = S_n^{(0)}(t)$ of Eq. (2.10). Solid (dashed) lines correspond to solution III (II) of Ref. 22.

where

$$S_n^{(k)}(t) = 2\nu_N^{2k+1}\gamma_n + \frac{2}{\pi}\int_{\bar{\nu}}^{N} d\nu\, \nu(\nu^2 - \bar{\nu}^2)^k \mathrm{Im}\, M_n(\nu, t)\,. \tag{2.12}$$

For $\nu \gg N$ (which is the case in all subsequent calculations) we find it is sufficiently accurate to keep only the leading term ($k=0$) in the sum. Subsequently, we set

$$S_n \equiv S_n^{(0)}(t)\,. \tag{2.13}$$

In this approach, once the effective Regge exponents $\alpha_n(t)$ are fixed, there are two unknown real functions: $b_0(t)$ and $b_1(t)$. These are determined in terms of the experimental differential cross section $d\sigma/dt$ and polarization P at a given high energy (inputs) by means of Eqs. (2.3), (2.4), and the above expressions for $\mathrm{Im}\, M_n$ and $\mathrm{Re} M_n$. Then the t structure of the amplitudes is completely specified.

In Fig. 1 we present the functions $S_0(t)$ and $S_1(t)$ used in our calculations (solid lines). These have been determined on the basis of the phase-shift analysis of Ref. 22. This analysis extends up to $E = 2$ GeV and presents four different solutions, I, II, III, and IV. The solid lines of Fig. 1 correspond to solution III, which has been selected because $S_1(t)$ changes sign near $t = -0.55$ (in accord with well-known dual-absorptive requirements). To test the stability of our results, throughout all this work (Sec. II and Sec. III) we have also carried calculations with the solution II of Ref. 22 (the corresponding $S_0(t)$ and $S_1(t)$ are shown in Fig. 1 with dashed lines); and we have found that our amplitudes remain practically unaffected.

In the calculation of this section we have used the following effective Regge trajectories:

$$\alpha_0(t) = 0.45 + 0.8t + 0.03t^2\,,$$
$$\alpha_1(t) = 0.45 + 0.9t + 0.03t^2\,. \tag{2.14}$$

We used as input the differential cross-section data at $E = 5.9$ GeV and we varied $\alpha_0(t)$ and $\alpha_1(t)$ (within reasonable limits) until we achieved a fit to all $d\sigma/dt$ data in the range $5.9 \leq E \leq 199.3$ GeV (Fig. 2, solid lines). In particular, at the highest

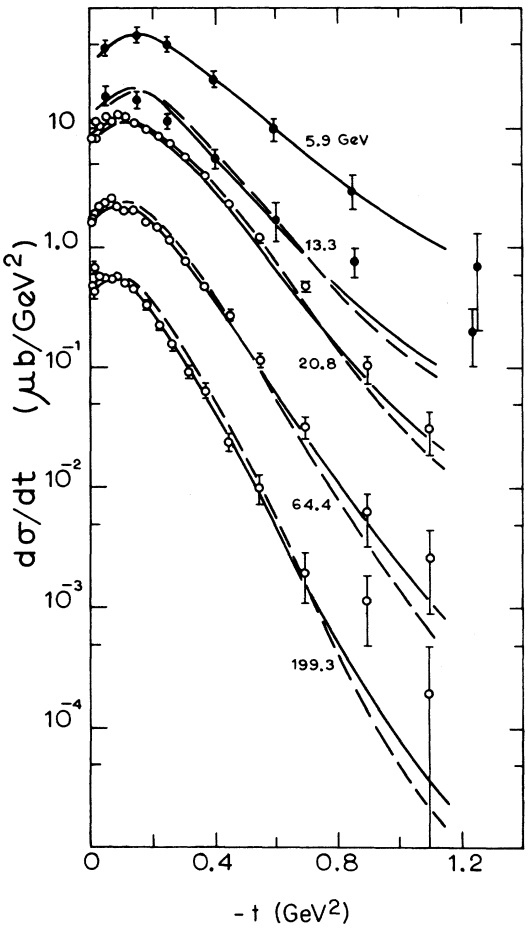

FIG. 2. Differential cross sections for $\pi^- p \to \eta n$. Data: ○ Ref. 12, ● O. Guisan *et al.*, Phys. Lett. 18, 200 (1965). Solid lines: calculations of the OETA (Sec. II); dashed lines: calculations of the TRPA (Sec. III).

Fermilab energies the fit is very sensitive to the exact form of $\alpha_0(t)$ and $\alpha_1(t)$; however, the t structure of the resulting amplitudes is much less sensitive.[15] Our effective trajectories are not too far from the "experimental" effective trajectory.[12]

$$\alpha(t) = 0.371 \pm 0.008 + (0.79 \pm 0.04)t + (0.03 \pm 0.04)\, t^2 .$$

Our effective trajectories vanish in the region $|t| \simeq 0.5$–0.6 GeV^2. Since Eq. (2.7) contains the term $\cot(\pi\alpha_n/2)$, which diverges at $\alpha_n = 0$ in our calculations, we have written the effective residue functions $b_n(t)$ of (2.5) in the form

$$b_n(t) = \alpha_n(t) g_n(t) . \tag{2.15}$$

The polarization data[19-21] are imprecise, and in some cases different experiments seem to disagree. All high-energy data are consistent with very small polarization P. We have varied widely our input P (within the experimental limits), but our approach gives real solutions for $b_0(t)$ and $b_1(t)$ only when $|P| \lesssim 0.03$, i.e., when the input polarization is practically zero. This point is further discussed in Sec. III and Sec. V.

The nonflip and flip SHA at $E = 5.9$ GeV corresponding to zero polarization are presented in Fig. 3. One of the basic features of all the SHA determined by the OETA is that they are very smooth functions of t in the whole range of our amplitude analysis. Further discussion of their features is postponed until Sec. IV.

In general, the DR approach we follow in this section leads to more than one solution for $b_n(t)$ (Refs. 4, 14, 16). The solution corresponding to the amplitudes of the Fig. 3 has been chosen by requiring the best possible agreement with FESR. For $\pi^- p \to \eta n$ the FESR of moment k has the form

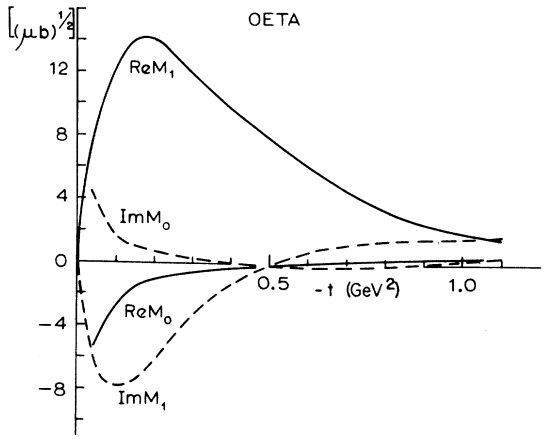

FIG. 3. The SHA in the one-effective-trajectory approach (OETA) at $E = 5.9$ GeV.

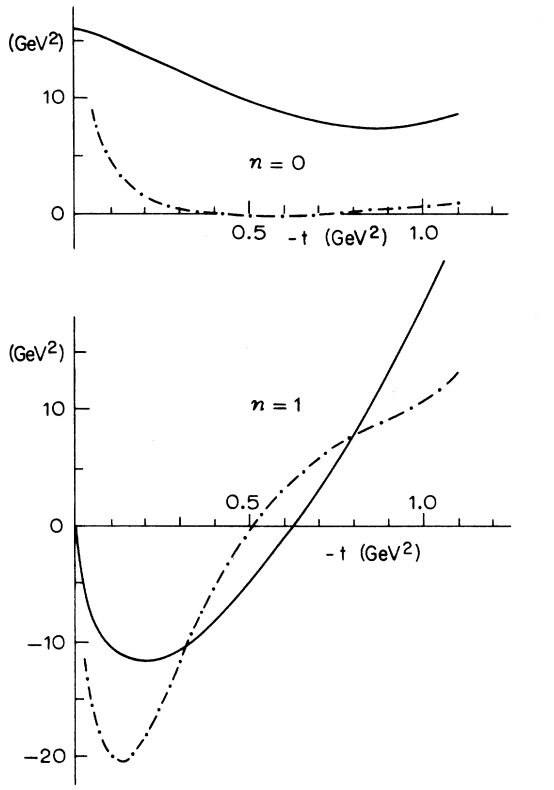

FIG. 4. Comparison with lowest-moment FESR in the OETA [Eq. (2.16) for $k = 0$]. Solid lines: right-hand side of Eq. (2.16); dashed lines: left-hand side of (2.16).

[see the right-hand side of Eq. (2.11)]

$$\frac{2}{\pi} \frac{b_n(t)}{\alpha_n(t) + 2 + 2k} (N^2 - \bar{\nu}^2)^{\alpha_n/2+1+k} = S_n^{(k)}(t) . \tag{2.16}$$

For the lowest moment ($k = 0$) the left-hand side of the last relation is compared to $S_n^{(0)} = S_n(t)$ in Fig. 4. Although agreement is certainly not perfect, we see that our solution is in qualitative accord with FESR. Agreement seems to be better for the flip amplitude ($n = 1$) than for the nonflip ($n = 0$). Notice that this is much the same situation as for the vector-exchange amplitudes.[4,14-16]

III. THE TWO-REGGE-POLES APPROACH (TRPA)

Here we turn to an amplitude analysis of $\pi^- p \to \eta n$ by means of two Regge-pole exchanges, $\alpha(t)$ and $\alpha'(t)$. The SHA at high energy take the form

$$M_n(\nu, t) = \beta_n(t) \left(-\cot\frac{\pi\alpha}{2} + i\right) (\nu^2 - \bar{\nu}^2)^{\alpha/2} + \beta_n'(t) \left(-\cot\frac{\pi\alpha'}{2} + i\right) (\nu^2 - \bar{\nu}^2)^{\alpha'/2} \tag{3.1}$$

with $\bar{\nu}$ given in (2.6). The FESR for the lowest moment $k = 0$ becomes

$$\frac{2}{\pi}\frac{\beta_n(t)}{\alpha+2}(N^2-\bar{\nu}^2)^{\alpha/2+1}+\frac{2}{\pi}\frac{\beta_n'(t)}{\alpha'+2}(N^2-\bar{\nu}^2)^{\alpha'/2+1}=S_n(t)\,. \tag{3.2}$$

In this section we proceed as follows: We use the last equation to determine $\beta_n'(t)$ in terms of $\beta_n(t)$ and $S_n(t)$. Then with the trajectories $\alpha(t)$ and $\alpha'(t)$ specified, all $\mathrm{Re}\,M_n(\nu,t)$ and $\mathrm{Im}\,M_n(\nu,t)$ depend on two unknown real functions, $\beta_0(t)$ and $\beta_1(t)$. These functions are determined by means of input data on $d\sigma/dt$ and P at a given high energy. Clearly, in this way the lowest-moment FESR, Eq. (3.2), are satisfied *exactly*.

Again we use as input the differential cross section data at $E=5.9$ GeV. As in Sec. II, the fit to all $d\sigma/dt$ in the range $5.9\le E\le 199.3$ GeV is sensitive to the exact value of α and α'. For simplicity here we use straight-line trajectories, and we have found that the forms

$$\alpha(t)=0.43+0.81t\,,\quad \alpha'(t)=-0.1+0.72t \tag{3.3}$$

give a reasonable fit to the $d\sigma/dt$ data (Fig. 2, dashed lines). Thus our leading trajectory α is close to the ρ-A_2 exchange-degenerate trajectory of several Regge analyses. On the other hand our nonleading trajectory $\alpha'(t)$ is not far from the nonleading ρ' trajectory of Barger and Phillips.[17]

As in Sec. II, because of the fact that $\cot(\pi\alpha/2)=\infty$ at $t=-0.53$ GeV^2 in our calculations we have written the A_2 residue functions in the form

$$\beta_n(t)=\alpha(t)\gamma_n(t)\,. \tag{3.4}$$

Again we use the functions $S_0(t)$ and $S_1(t)$ shown with solid lines in Fig. 1 (solution III of Ref. 22).

Also owing to the even signature of the trajectory of A_2, taken literally, the contribution of $\alpha'(t)$ of (3.3) would imply the existence of a spin-0 particle of mass ~0.374 GeV. However, our analysis has no implications for $t>0$, and such unwanted objects can easily be eliminated by properly making the residue functions $\beta_n'(t)$ vanish at $t\simeq 0.14$.

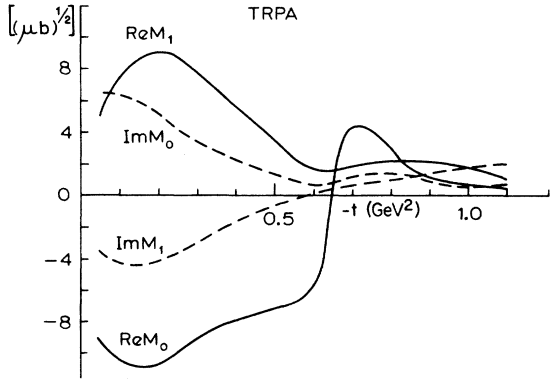

FIG. 5. The SHA in the two-Regge-poles approach (TRPA) at $E=5.9$ GeV.

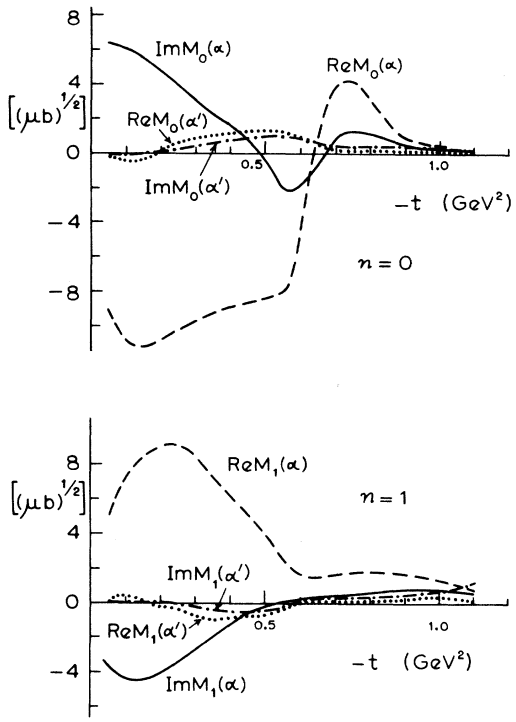

FIG. 6. Separate contributions to SHA in the TRPA from the leading trajectory $\alpha(t)$ and the nonleading $\alpha'(t)$. Solid lines: $\mathrm{Im}\,M_n(\alpha)$; dashed lines: $\mathrm{Re}M_n(\alpha)$; dash-dotted lines: $\mathrm{Im}\,M_n(\alpha')$; dotted lines: $\mathrm{Re}M_n(\alpha')$.

It is very remarkable that in the present approach as well, in spite of using two well-separated trajectories $\alpha(t)$ and $\alpha'(t)$, we obtain real solutions for $\beta_0(t)$ and $\beta_1(t)$ only when the polarization $|P|$ is *very small* (here $|P|<0.05$). Therefore we proceed in our amplitude analysis using again zero polarization.

The nonflip and flip SHA of this calculation at $E=5.9$ GeV are given in Fig. 5. In the present approach (TRPA) the imaginary parts of the SHA are again smooth functions of t (as in the one-effective-trajectory approach of Sec. II); their t structure is determined, to a great extent, by the t structure of the input functions $S_0(t)$ and $S_1(t)$ and by the condition of Eq. (3.2) (satisfaction of FESR). However, the real parts of the SHA show significant variation in t. In particular, $\mathrm{Re}M_0$ changes sign and shows much variation around $t\simeq -0.6$ GeV^2, and this feature is understood as follows: Notice first that near $t\simeq -0.5$ we obtain real solutions for $\beta_n(t)$ only when $|P|<0.05$; hence, as we already stressed, our approach demands $P\approx 0$. On the other hand the input $d\sigma/dt$ is smooth (and fairly large) around $|t|=0.5$–0.6. Now, the

input $S_1(t)$ and therefore also $\mathrm{Im}M_1(t)$ change sign at $t \simeq -0.5$; however, $S_0(t)$ and $\mathrm{Im}M_0(t)$ stay positive. Also, $\mathrm{Re}M_1(t)$ stays positive [as can be seen from the shape of $\mathrm{Im}M_1(t)$ and the $\cot(\pi\alpha/2)$ factors]. Then, to obtain $P \approx 0$ and $d\sigma/dt$ large, $\mathrm{Re}M_0(t)$ has to vary significantly, and change sign in this region of t.

In Fig. 6 we present separately the contributions to $\mathrm{Re}M_n$ and $\mathrm{Im}M_n$ from each of the exchanges $\alpha(t)$ and $\alpha'(t)$. We remark that at small $|t|$ the contribution of $\alpha'(t)$ to both M_0 and M_1 is small compared to that of $\alpha(t)$. At large $|t|$ the contribution of $\alpha'(t)$ becomes more significant, in particular to the nonflip $\mathrm{Im}M_0$.

IV. AMPLITUDE STRUCTURE—EXCHANGE DEGENERACY

The basic difference in the results of the OETA (Fig. 3) and of the TRPA (Fig 5) is the relative magnitude of the nonflip M_0 and the flip M_1 SHA. In the first case, in general, $|M_0|$ is significantly smaller than $|M_1|$, as is usually believed for $\pi^- + p \to \eta + n$; in the second case $|M_0|$ and $|M_1|$ are comparable, at least around $|t| \simeq 0.2$–0.3 GeV^2. Another difference is in the overall shape of $\mathrm{Re}M_0(t)$.

In spite of the differences, however, there are several similarities in the t structure of the SHA.

First, in both cases the imaginary part of the nonflip SHA, $\mathrm{Im}M_0(t)$, differs significantly from the DAM form $\sim J_0(R\sqrt{-t})$, $R \simeq 1$ fermi. This is the conclusion of a number of amplitude analyses involving tensor exchange[1-10] and is well supported by both approaches of the present analysis. Also, in both cases we find that $\mathrm{Im}M_0(t)$ has a minimum in the region $|t| \simeq 0.5$–0.6.

Second, the imaginary part of the flip, $\mathrm{Im}M_1(t)$, is clearly of the DAM form $\sim J_1(R\sqrt{-t})$. However, this features is a result of our procedures rather than a prediction. In Sec. II it is the result of writing the residues in the form $b_1(t) = \alpha_1(t) g_1(t)$ [Eq. (2.15)], and in Sec. III it is a result of satisfying the FESR (3.2) and of having the input function $S_1(t)$ with a change of sign at $t \simeq -0.5$ GeV^2.

Third, the real part of the nonflip, $\mathrm{Re}M_0(t)$, although it differs in overall magnitude and shape, does have in common the feature of changing sign at $|t| \simeq 0.5$–0.6 GeV^2 in both cases. This change of sign of $\mathrm{Re}M_0$ has also been observed in many amplitude analyses involving tensor exchange.[4,10]

Finally, the real part of the flip, $\mathrm{Re}M_1(t)$, shows no change of sign and stays relatively large at $|t| \simeq 0.5$–0.6 GeV^2 in both approaches.

Recently we have received an amplitude analysis involving A_2 exchange[23] in which a parametrization of the ρ and A_2 amplitudes is used to fit available data on $\pi^- + p \to \pi^0 + n$, $\pi^- + p \to \eta + n$, $K^- + p \to \bar{K}^0 + n$, $K^+ + n \to K^0 + p$. Although the approach is quite different from ours, the resulting A_2 SHA show all the above-mentioned features for both nonflip and flip. The SHA of Ref. 23 are particularly similar to our Fig. 3 (OETA).

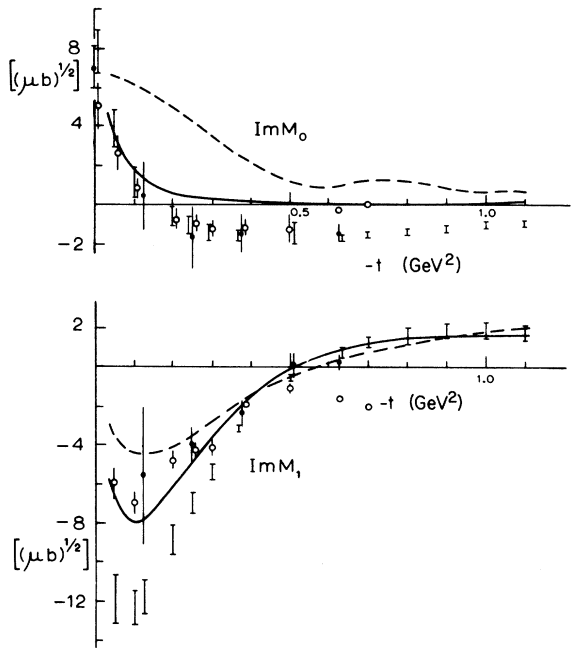

FIG. 7. Exchange degeneracy between A_2 and ρ at $E = 5.9$ GeV. $-A_2$ exchange contribution ($\pi^- p \to \eta n$): solid lines, OETA, dashed lines, TRPA; $-\rho$ exchange contribution ($\pi^- p \to \pi^0 n$): ● Ref. 24, I Ref. 25, ○ Ref. 26.

An important question, over which there has been much controversy, is the exchange degeneracy (EXD) between A_2 and ρ exchange amplitudes, and specifically between the imaginary parts of the SHA for A_2 and ρ.[11]

To answer this we plot in Fig. 7 our $\mathrm{Im}M_n(t)$ at $E = 5.9$ GeV of OETA (solid lines) and of TRPA (dashed lines). In the same figure we plot the imaginary parts of the SHA as they have been determined in a number of model-independent amplitude analyses[24,25,26] (within an arbitrary t-dependent phase).

With respect to the nonflip amplitude, at small $|t|$ ($\lesssim 0.3$ GeV^2) we see that $\mathrm{Im}M_0(t)$ of our OETA is exchange-degenerate with the $\mathrm{Im}M_0$ of ρ exchange; the $\mathrm{Im}M_0(t)$ of TRPA is somewhat larger. At larger $|t|$, however, we find no EXD; this is a result of the fact that the $\mathrm{Im}M_0$ corresponding to tensor exchange (A_2) deviates from the DAM form $\sim J_0(R\sqrt{-t})$, whereas the $\mathrm{Im}M_0$ of vector exchange (ρ) is quite consistent with DAM.

With respect to the flip amplitude, for ρ exchange the results of the amplitude analyses differ. If we accept the analyses of Refs. 24 and 25, our

solutions for $\mathrm{Im}M_1$ of A_2 are in fair agreement with EXD. The analysis of Ref. 26 gives $\mathrm{Im}M_1(\rho)$ in accord with $\mathrm{Im}M_1(A_2)$ of TRPA at $|t| \lesssim 0.5$; however, at larger $|t|$, $\mathrm{Im}M_1$ of Ref. 26 deviates from the DAM form and therefore violates EXD. As is well known, the difference in $\mathrm{Im}M_1(\rho)$ between the amplitude analysis of Ref. 26 and Refs. 24 and 25 is due to different input polarization for $\pi^- + p \to \pi^0 + n$ (ANL vs CERN).

We may conclude that if we accept the amplitude analyses of Refs. 24 and 25 (CERN polarization), on the whole the imaginary parts of our SHA do satisfy EXD, $\mathrm{Im}M_1$ for all t and $\mathrm{Im}M_0$ for $|t| \lesssim 0.3$ GeV^2.

V. SPIN ROTATIONAL PARAMETER—DISCUSSION OF POLARIZATION

To further distinguish between our two approaches (OETA versus TRPA) we have calculated the spin rotational parameter

$$T = \frac{2\,\mathrm{Re}(M_0 M_1^*)}{|M_0|^2 + |M_1|^2} . \tag{5.1}$$

In principle this parameter can be determined experimentally and will allow a distinction between the SHA of Fig. 3 and Fig. 5.

The results of our calculation at $E = 5.9$ GeV are shown in Fig. 8. There is a clear difference in the predicted T for all $|t| \gtrsim 0.2$ GeV^2. In the OETA (solid line) $|T|$ is smooth and very small for $|t| \gtrsim 0.2$. In the TRPA (dashed line) $|T|$ is generally large and shows a dramatic change near $t \simeq -0.6$ GeV^2. This is easily traced in the different structure of $\mathrm{Re}M_0(t)$.

We would like to conclude with certain comments on the fact that both OETA and TRPA required very small input polarization P. Clearly both our approaches rely on the input functions $S_n(t)$ determined from the phase-shift analysis of Ref. 22. It would be highly desirable to use input $S_n(t)$ arising from other phase-shift analyses (of other authors) as well. Unfortunately we have been unable to make effective use of any other analysis of

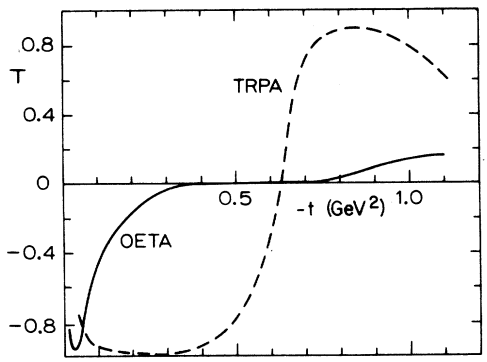

FIG. 8. Predictions for the spin rotational parameter T, Eq. (4.1), at $E = 5.9$ GeV. Solid line, OETA; dashed line, TRPA.

$\pi^- + p \to \eta + n$. Anyway, as stated in Sec. II, Ref. 22 presents four somewhat different solutions, and we have obtained very similar results by using different $S_n(t)$.

Now *accepting* the $S_n(t)$ of Ref. 22 we can say that the demand $P \approx 0$ in our work is not unrelated to the analyticity requirements [in the variable $\nu = (s-u)/4M$] which we impose in our solutions: In the OETA we make direct use of fixed-t DR Eq. (2.4), and in the TRPA analyticity is satisfied via the FESR Eq. (3.2). We may conclude that the input $d\sigma/dt$ and $S_n(t)$ together with the analyticity requirements lead in the present case to $P \approx 0$.

We note that the recent analysis of Ref. 23 also predicts small polarization for $\pi^- p \to \eta n$ at all t; their maximum (at $t \simeq -0.2$ GeV^2) is $P = 0.2$.

For all these reasons more accurate polarization data for $\pi^- p \to \eta n$ will be of much interest. We may hope that they will be available in the not-too-distant future.

ACKNOWLEDGMENTS

We would like to thank Bob Gaskell for discussions and for help in the calculations.

†Work supported in part by the National Research Council of Canada.

[1] V. D. Barger, in *Proceedings of the XVII International Conference on High Energy Physics, London, 1974* edited by J. R. Smith (Rutherford Laboratory, Chilton, Didcot, Berkshire, England, 1974), p. I-193.
[2] V. D. Barger, K. Geer, and F. Halzen, Nucl. Phys. B49, 302 (1972).
[3] V. D. Barger (Ref. 1), p. I-214.
[4] E. Argyres, A. P. Contogouris, M. Svec, and S. Ray, Ann. Phys. (N.Y.) 85, 283 (1974).
[5] V. D. Barger and A. D. Martin, Phys. Lett. B39, 379 (1972).
[6] A. Irving, A. D. Martin, and V. D. Barger, Nuovo Cimento A16, 573 (1973).
[7] E. Argyres, A. P. Contogouris, and J. P. Holden, Phys. Rev. D 9, 1340 (1974).
[8] G. Girardi, C. Godreche, and H. Navelet, Nucl. Phys. B76, 541 (1974).
[9] F. Elvekjaer and R. Johnson, Nucl. Phys. B83, 127 (1974); B83, 142 (1974).
[10] E. Argyres, A. P. Contogouris, and J. P. Holden, Phys. Rev. D 10, 2095 (1974).
[11] R. Worden, in *Proceedings of the XVII International Conference on High Energy Physics, London, 1974* (Ref. 1), p. I-153.

[12]O. Dahl *et al.*, Phys. Rev. Lett. 37, 80 (1976).
[13]L. Wolfenstein, Phys. Rev. 96, 1654 (1954).
[14]E. Argyres, A. P. Contogouris, J. P. Holden, and M. Svec, Phys. Rev. D 8, 2068 (1973).
[15]M. Svec, Ph.D. thesis, McGill University, 1976 (unpublished).
[16]A. P. Contogouris, Can. J. Phys. 54, 390 (1976).
[17]V. D. Barger and R. J. N. Phillips, Phys. Rev. 187, 2210 (1969).
[18]V. D. Barger and R. J. N. Phillips, Phys. Lett. B53, 195 (1974).
[19]P. Bonamy *et al.*, Nucl. Phys. B16, 335 (1970).
[20]P. Bonamy *et al.*, Nucl. Phys. B52, 392 (1973).
[21]D. Drobnis *et al.*, Phys. Rev. Lett. 20, 274 (1968).
[22]C. Botke, Phys. Rev. 180, 1417 (1969).
[23]H. Navelet and P. Stevens, Nucl. Phys. B118, 475 (1977).
[24]F. Halzen and C. Michael, Phys. Lett. B36, 367 (1971).
[25]R. L. Kelly, Phys. Lett. B39, 635 (1971).
[26]P. Johnson *et al.*, Phys. Rev. Lett. 30, 242 (1973).